Localized modes in two-dimensional square anisotropic antiferromagnets with a hole

Mari Kubota and Kazuko Kawasaki
Department of Physics, Nara Women's University, Nara 630-8506, Japan

Shozo Takeno
Department of Information Systems, Osaka Institute of Technology, Hirakata, Osaka 573-01, Japan

(Received 1 September 1999; revised manuscript received 22 August 2000; published 31 January 2001)

A theory of localized modes in two-dimensional square anisotropic ferromagnets with a hole is extended to the antiferromagnetic case. Here a path-integral method based on the SU(2) coherent state representation is employed. Detailed numerical calculations are made for *s*-like modes, and their eigenfrequency is determined as a function of nonlinearity parameter and various anisotropic exchange interactions and uniaxial anisotropies. Particular attention is paid to interplaying between the intrinsic nonlinearity and extrinsic hole doping. It turns out that the former stabilizes the magnetic localized mode generated by the latter (or vice versa), and it takes a vortex shape in the neighborhood of a doped hole. In contrast to the ferromagnetic case, the mobile nonlinear self-localized mode is unlikely to exist.

DOI: 10.1103/PhysRevB.63.094407 PACS number(s): 75.30.Ds

I. INTRODUCTION

Recently, we developed a path-integral formulation in SU(2) coherent-state representation of self-localized modes for two-dimensional (2D) Heisenberg ferromagnet containing a fixed magnetic hole.[1] For *s*-like modes, expressions for the energy eigenvalues and profile functions of the localized modes were obtained in terms of Green's functions. By using analytical and numerical methods, both effects were studied in detail to obtain stationary, immobile localized modes and mobile ones.

In this paper we study a 2D Heisenberg antiferromagnet bearing a fixed magnetic hole, in the same spirit as that in the previous paper for the ferromagnet. Our particular concern here is whether or not there exists any situations for the properties of intrinsic localized modes that are different from the case of the ferromagnets. This paper is organized as follows. In the next section, a brief account is given on the SU(2) coherent-state path-integral formalism for antiferromagnet. By employing the stationary phase approximation a pair of nonlinear equations are derived. In Sec. III, the outline of studying the nonlinear eigenvalue problem with magnon Green's functions is described. Numerical illustrations are made for an *s*-like self-localized mode in Sec. IV. Their eigenfrequencies and spin profiles are analyzed as a function of nonlinearity parameter for various anisotropic exchange interactions and uniaxial anisotropies. The last section, Sec. V, is devoted to concluding remarks on the results obtained in this paper.

II. SU(2) COHERENT-STATE PATH-INTEGRAL FORMULATION AND STATIONARY PHASE APPROXIMATION

We consider a Heisenberg antiferromagnet on a 2D square lattice with the lattice constant $a=1$. The Hamiltonian can be written in the form

$$H=\sum_{\langle nm\rangle} J(n,m)[\eta(S_n^+S_m^-+S_n^-S_m^+)+S_n^zS_m^z]$$
$$-D\left[\sum_n (S_n^z)^2+\sum_m (S_m^z)^2\right], \tag{1}$$

where S_n^α $(\alpha=x,y,z)$ is the α component of the nth site spin operator situated on the lattice vector $\boldsymbol{n}=n_x\boldsymbol{e}_x+n_y\boldsymbol{e}_y$ with an unit vector $\boldsymbol{e}_j$ in the direction of the j axis. The $J(n,m)(>0)$, $\eta(>0)$ and $D(>0)$ are exchange interaction constant between neighboring sites n and m, a constant characterizing the anisotropy of the exchange interaction and the uniaxial crystal-field anisotropy parameter, respectively. The symbol $\Sigma_{\langle nm\rangle}$ indicates the sum over nearest-neighbor pairs. Assuming that the lattice is bipartite and divided into A and B sublattices, the SU(2) coherent states $|\mu_n\rangle$ and $|\nu_m\rangle$ are defined by using the Néel state $|0\rangle$ as

$$|\mu_n\rangle=(1+|\mu_n|^2)^{-S}\exp(\mu_nS_n^-)|0\rangle_n,$$
$$\text{for}\ \ n\in A\ \ \text{sublattice}, \tag{2}$$

$$|\nu_m\rangle=(1+|\nu_m|^2)^{-S}\exp(\nu_mS_m^+)|0\rangle_m,$$
$$\text{for}\ \ m\in B\ \ \text{sublattice}, \tag{3}$$

where the μ_n's and ν_m's are complex magnon field variables associated with the A and B sublattices, respectively. The diagonal coherent-state representations of the spin operator $\boldsymbol{S}_n$ are given by

$$\langle\mu_n|S_n^+|\mu_n\rangle=2S\frac{\mu_n}{1+|\mu_n|^2},\ \ \langle\mu_n|S_n^-|\mu_n\rangle=2S\frac{\mu_n^*}{1+|\mu_n|^2},$$

$$\langle\mu_n|S_n^z|\mu_n\rangle=S\frac{1-|\mu_n|^2}{1+|\mu_n|^2}, \tag{4}$$

$$\langle\nu_m|S_m^+|\nu_m\rangle=2S\frac{\nu_m^*}{1+|\nu_m|^2},$$

$$\langle\nu_m|S_m^-|\nu_m\rangle=2S\frac{\nu_m}{1+|\nu_m|^2},\ \ \langle\nu_m|S_m^z|\nu_m\rangle=-S\frac{1-|\nu_m|^2}{1+|\nu_m|^2}.$$

According to path-integral theory,[2,3] the transition amplitude of the system from the initial state $|\Lambda_i\rangle$ at the time t_i to the final state $|\Lambda_f\rangle$ at the time t_f is given by the functional-integral representation for the matrix element of the evolution operator $\exp(-iHt/\hbar)$,[4,3]

$$\langle\Lambda_f|\exp[-iH(t_f-t_i)/\hbar]|\Lambda_i\rangle=\int\mathcal{D}(\Lambda)\exp(iS/\hbar),\tag{5}$$

with

$$S=\int_{t_i}^{t_f}\mathcal{L}dt,\tag{6}$$

where the Lagrangian $\mathcal{L}$ is defined by

$$\mathcal{L}=\sum_n\frac{S}{1+|\mu_n|^2}\left(\mu_n^*i\hbar\frac{d\mu_n}{dt}-\mu_n i\hbar\frac{d\mu_n^*}{dt}\right)+\sum_m\frac{S}{1+|\nu_m|^2}\left(\nu_m^*i\hbar\frac{d\nu_m}{dt}-\nu_m i\hbar\frac{d\nu_m^*}{dt}\right)-\langle\Lambda|H|\Lambda\rangle.\tag{7}$$

Here the functional integration involving the symbol $\mathcal{D}(\Lambda)$ in Eq. (5) means a sum over all paths moving forward in time t. An explicit expression for $\langle\Lambda|H|\Lambda\rangle$ in Eq. (7) is given by

$$\begin{aligned}\langle\Lambda|H|\Lambda\rangle=&-S^2\sum_{\langle nm\rangle}J(n,m)\frac{1}{(1+|\mu_n|^2)(1+|\nu_m|^2)}\\&\times2\eta(\mu_n\nu_m+\mu_n^*\nu_m^*)-(1-|\mu_n|^2)(1-|\nu_m|^2)\\&-DS^2\left[\sum_n\left(\frac{1-|\mu_n|^2}{1+|\mu_n|^2}\right)^2+\sum_m\left(\frac{1-|\nu_m|^2}{1+|\nu_m|^2}\right)^2\right]\\&-2DS\left[\sum_n\frac{|\mu_n|^2}{(1+|\mu_n|^2)^2}+\sum_m\frac{|\nu_m|^2}{(1+|\nu_m|^2)^2}\right].\end{aligned}\tag{8}$$

In obtaining the above result, we have made use of the relation

$$\langle\lambda_l|(S_l^z)^2|\lambda_l\rangle-\langle\lambda_l|S_l^z|\lambda_l\rangle^2=\frac{2D|\lambda_l|^2}{(1+|\lambda_l|^2)^2},\ \ \lambda_l=\mu_n,\nu_m.\tag{9}$$

As a first-order approximation to the exact path-integral formalism described above, we employ the saddle-point approximation to Eq. (5), i.e., $\delta S=0$. Then, we arrive at the Lagrangian equations

$$\frac{d}{dt}\left(\frac{\partial\mathcal{L}}{\partial\dot{\mu}_n}\right)-\frac{\partial\mathcal{L}}{\partial\mu_n}=0,\quad-\frac{d}{dt}\left(\frac{\partial\mathcal{L}}{\partial\dot{\nu}_m}\right)-\frac{\partial\mathcal{L}}{\partial\nu_m}=0\quad\text{and c.c.}\tag{10}$$

Combining Eq. (7) with Eq. (10) gives a pair of equations:

$$i\hbar\frac{d\mu_n}{dt}=\frac{(1+|\mu_n|^2)^2}{2S}\frac{\partial\langle\Lambda|H|\Lambda\rangle}{\partial\mu_n^*},$$

$$-i\hbar\frac{d\nu_m^*}{dt}=\frac{(1+|\nu_m|^2)^2}{2S}\frac{\partial\langle\Lambda|H|\Lambda\rangle}{\partial\nu_m}\quad\text{and c.c.}\tag{11}$$

Inserting Eq. (8) into Eq. (11), we obtain nonlinear differential difference equations satisfied by the μ_n's and ν_m's,

$$i\hbar\dot{\mu}_n=K\mu_n+S\eta\sum_m J(n,m)\nu_m^*-V_1(\mu_n,\nu_m),\tag{12}$$

$$i\hbar\dot{\nu}_m^*=K\nu_m^*+S\eta\sum_m J(n,m)\mu_n-V_2(\nu_m,\mu_n),\tag{13}$$

where

$$K=zSJ+(2S-1)D,\tag{14}$$

in which $z(=4)$ is the number of nearest neighbors seen by a given spin. Here all the nonlinearity terms are incorporated into the factors $V_1(\mu_n,\nu_m)\equiv V_1$ and $V_2(\nu_m,\mu_n)\equiv V_2$. Their explicit expressions are given by

$$V_1=S\sum_m J(n,m)\frac{1}{1+|\nu_m|^2}[\eta(\mu_n^2\nu_m+|\nu_m|^2\nu_m^*)+2\mu_n|\nu_m|^2]+zSJ(n,m)D^*\frac{|\mu_n|^2\mu_n}{1+|\mu_n|^2},\tag{15}$$

$$V_2=S\sum_n J(n,m)\frac{1}{1+|\mu_n|^2}[\eta(\mu_n^*\nu_m^*+\mu_n|\mu_n|^2)+2\nu_m^*|\mu_n|^2]+zSJ(n,m)D^*\frac{|\nu_m|^2\nu_m}{1+|\nu_m|^2},\tag{16}$$

with

$$D^*=\frac{2(2S-1)}{zSJ}D.\tag{17}$$

This is a modified version of the nonlinear Schrödinger equation,[5] in which intrinsic nonlinearity of the spin system has been included to all orders. Corrections to the saddle-point approximation by considering quantum fluctuations around the stationary point would be required, because this approximation works better for $S\gg1$.

III. OUTLINE OF STUDYING NONLINEAR EIGENVALUE PROBLEMS

We study nonlinear eigenvalue problems associated with Eqs. (12) and (13). This amounts to seeking solutions to these equations in the form

$$\mu_n = |\mu_n|\exp(-i\omega t) \equiv \frac{\mathcal{A}}{\sqrt{2S}}\xi(\boldsymbol{n})\exp(-i\omega t), \tag{18}$$

$$\nu_m = |\nu_m|\exp(-i\omega t) \equiv \frac{\mathcal{A}}{\sqrt{2S}}\zeta(\boldsymbol{m})\exp(i\omega t). \tag{19}$$

Here the quantities ω and $\xi(\boldsymbol{n})$ $[\zeta(\boldsymbol{m})]$ are the eigenfrequency of the stationary nonlinear modes to be studied and the envelope functions for A (B) sublattice which is assumed to be time independent. The quantity A is the reduced amplitude of the nonlinear modes. We are principally concerned here with subtle interplaying of the intrinsic nonlinearity in magnons and the extrinsic disorder due to hole doping. For convenience, we divide our procedure of studying the nonlinear eigenvalue problems into three steps as given below.

(i) *Pure nonlinear system.* We first consider a pure 2D square antiferromagnet with nearest-neighbor coupling constant $J(n,m)=J$ for all n and m. Then, substituting Eqs. (18) and (19) to Eqs. (12) and (13) leads to

$$\frac{\overline{K}-\overline{E}}{\eta}\xi(\boldsymbol{n}) + \frac{1}{2}\sum_{j=x,y}[\zeta(\boldsymbol{n}+\boldsymbol{e}_j)+\zeta(\boldsymbol{n}-\boldsymbol{e}_j)] = \frac{\lambda}{2\eta}\mathcal{U}_1(\xi,\zeta), \tag{20}$$

$$\frac{\overline{K}+\overline{E}}{\eta}\zeta(\boldsymbol{m}) + \frac{1}{2}\sum_{j=x,y}[\xi(\boldsymbol{m}+\boldsymbol{e}_j)+\xi(\boldsymbol{m}-\boldsymbol{e}_j)] = \frac{\lambda}{2\eta}\mathcal{U}_2(\zeta,\xi), \tag{21}$$

where

$$\overline{E} = \frac{\hbar\omega}{2SJ} = \frac{E}{2SJ}, \quad \overline{K} = \frac{K}{2SJ} = \frac{4SJ+(2S-1)D}{2SJ} = 2 + D^*, \tag{22}$$

$$\mathcal{U}_1(\xi,\zeta) = \sum_{j=x,y}\left(D^*\frac{\xi(\boldsymbol{n})^3}{1+\lambda\xi(\boldsymbol{n})^2} + \frac{2\zeta(\boldsymbol{n}+\boldsymbol{e}_j)^2\xi(\boldsymbol{n}) + \eta\zeta(\boldsymbol{n}+\boldsymbol{e}_j)[\xi(\boldsymbol{n})^2+\zeta(\boldsymbol{n}+\boldsymbol{e}_j)^2]}{1+\lambda\zeta(\boldsymbol{n}+\boldsymbol{e}_j)^2} + \frac{2\zeta(\boldsymbol{n}-\boldsymbol{e}_j)^2\xi(\boldsymbol{n}) + \eta\zeta(\boldsymbol{n}-\boldsymbol{e}_j)[\xi(\boldsymbol{n})^2+\zeta(\boldsymbol{n}-\boldsymbol{e}_j)^2]}{1+\lambda\zeta(\boldsymbol{n}-\boldsymbol{e}_j)^2}\right), \tag{23}$$

$$\mathcal{U}_2(\zeta,\xi) = \sum_{j=x,y}\left(D^*\frac{\zeta(\boldsymbol{m})^3}{1+\lambda\zeta(\boldsymbol{m})^2} + \frac{2\xi(\boldsymbol{m}+\boldsymbol{e}_j)^2\zeta(\boldsymbol{m}) + \eta\xi(\boldsymbol{m}+\boldsymbol{e}_j)[\zeta(\boldsymbol{m})^2+\xi(\boldsymbol{m}+\boldsymbol{e}_j)^2]}{1+\lambda\xi(\boldsymbol{m}+\boldsymbol{e}_j)^2} + \frac{2\xi(\boldsymbol{m}-\boldsymbol{e}_j)^2\zeta(\boldsymbol{m}) + \eta\xi(\boldsymbol{m}-\boldsymbol{e}_j)[\zeta(\boldsymbol{m})^2+\xi(\boldsymbol{m}-\boldsymbol{e}_j)^2]}{1+\lambda\xi(\boldsymbol{m}-\boldsymbol{e}_j)^2}\right). \tag{24}$$

The parameter λ defined by

$$\lambda \equiv \mathcal{A}^2/2S, \tag{25}$$

characterizes the nonlinearity of the spin system.

(ii) *Linear impurity modes.* As a preliminary step for studying stationary nonlinear modes in a 2D antiferromagnet containing a hole, we consider a system containing an impurity spin located at the origin. As shown in Fig. 1, there exist two kinds of coupling constants; J' between an impurity at the origin and its nearest-neighbor sites and J among host spin sites. When nonlinear effects are discarded, this system leads to the following equations, corresponding to Eqs. (20) and (21) for pure case;

(a) for $\boldsymbol{n}=\boldsymbol{0}$,

$$\frac{2+D^*-\overline{E}}{\eta}\xi(\boldsymbol{0}) + \frac{1}{2}\sum_{j=x,y}[\zeta(+\boldsymbol{e}_j)+\zeta(-\boldsymbol{e}_j)] = W_1(\xi(\boldsymbol{0}),\zeta), \tag{26}$$

(b) for $\boldsymbol{n}=\pm\boldsymbol{e}_j$,

$$\frac{2+D^*+\overline{E}}{\eta}\zeta(\pm\boldsymbol{e}_j) + \frac{1}{2}\sum_{j=x,y}\xi(\pm\boldsymbol{e}_j+\boldsymbol{e}'_j)+\xi(\pm\boldsymbol{e}_j-\boldsymbol{e}'_j) = W_2(\zeta(\pm\boldsymbol{e}_j),\xi), \tag{27}$$

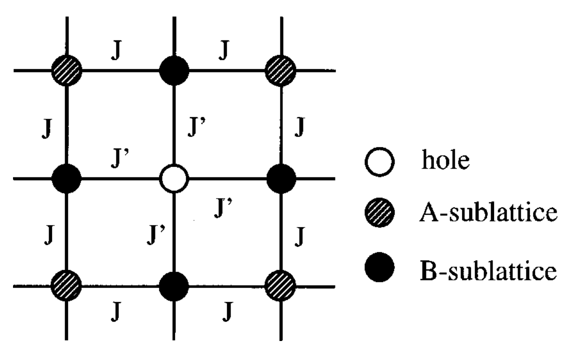

FIG. 1. Antiferromagnetic system with a hole fixed at the origin.

where

$$W_1(\xi(\mathbf{0}),\zeta)=\frac{(2+D^*)\Delta J}{\eta J}\xi(\mathbf{0})+\frac{\Delta J}{2J}\sum_{j=x,y}[\zeta(\mathbf{e}_j)+\zeta(-\mathbf{e}_j)], \tag{28}$$

$$W_2(\zeta(\pm\mathbf{e}_j),\xi)=\frac{\Delta J}{2\eta J}\zeta(\pm\mathbf{e}_j)+\frac{\Delta J}{2J}\xi(\mathbf{0}), \tag{29}$$

with

$$\Delta J=J-J', \tag{30}$$

(c) for other cases,

$$\frac{\overline{K}-\overline{E}}{\eta}\xi(\mathbf{n})+\frac{1}{2}\sum_{j=x,y}[\zeta(\mathbf{n}+\mathbf{e}_j)+\zeta(\mathbf{n}-\mathbf{e}_j)]=0, \tag{31}$$

$$\frac{\overline{K}+\overline{E}}{\eta}\zeta(\mathbf{m})+\frac{1}{2}\sum_{j=x,y}[\xi(\mathbf{m}+\mathbf{e}_j)+\xi(\mathbf{m}-\mathbf{e}_j)]=0. \tag{32}$$

It is understood that we eventually take the limit $J'\rightarrow 0$ or $\Delta J\rightarrow J$ to get the magnetic system with the hole. Then, Eqs. (28) and (29) take the form

$$W_1(\xi(\mathbf{0}),\zeta)=\frac{(2+D^*)}{\eta}\xi(\mathbf{0})+\frac{1}{2}\sum_{j=x,y}[\zeta(\mathbf{e}_j)+\zeta(-\mathbf{e}_j)], \tag{33}$$

$$W_2(\zeta(\pm\mathbf{e}_j),\xi)=\frac{1}{2\eta}\zeta(\pm\mathbf{e}_j)+\frac{1}{2}\xi(\mathbf{0}). \tag{34}$$

(iii) *Nonlinear impurity modes.* Our objective of obtaining stationary nonlinear modes for the present system can be achieved by introducing two linear operators L_0 and L',

$$\hat{L}_0\hat{\xi}\equiv\varepsilon\hat{\xi}(\mathbf{n})-\frac{1}{2}\sum_{j=x,y}[\hat{\xi}(\mathbf{n}+\mathbf{e}_j)+\hat{\xi}(\mathbf{n}-\mathbf{e}_j)], \tag{35}$$

and

$$\hat{L}'\hat{\xi}(\mathbf{n})\equiv\hat{W}(\xi,\zeta), \tag{36}$$

where

$$\varepsilon=\frac{\sqrt{(2+D^*)^2-\overline{E}^2}}{\eta}, \tag{37}$$

$$\hat{\xi}(\mathbf{n})=\begin{bmatrix}\xi(\mathbf{n})\\ \zeta(\mathbf{n})\end{bmatrix}\quad\text{and}\quad\hat{W}(\xi,\zeta)=\begin{bmatrix}W_1(\xi(\mathbf{0}),\zeta)\\ W_2(\zeta(\pm\mathbf{e}_j),\xi)\end{bmatrix}. \tag{38}$$

Namely, $\hat{L}_0$ is the operator for pure lattice and $\hat{L}'$ is the perturbations term due to the existence of a hole. Their explicit expressions are written as

$$\hat{L}_0=\begin{bmatrix}\frac{1}{\eta}(2+D^*-\overline{E}) & \sum_{j=x,y}\cosh\left(\frac{\partial}{\partial n_j}\right)\\ \sum_{j=x,y}\cosh\left(\frac{\partial}{\partial n_j}\right) & \frac{1}{\eta}(2+D^*+\overline{E})\end{bmatrix}, \tag{39}$$

and

$$\hat{L}'=\begin{bmatrix}\frac{1}{\eta}(2+D^*) & \frac{1}{\eta}\sum_{j=x,y}\cosh\left(\frac{\partial}{\partial n_j}\right)\\ \frac{1}{2} & \frac{1}{2}\exp\left(\pm\frac{\partial}{\partial n_j}\right)\end{bmatrix}. \tag{40}$$

By such a procedure, Eqs. (20) and (21) are replaced by

$$(\hat{L}_0-\hat{L}')\hat{\xi}(\mathbf{n})=\frac{\lambda}{2\eta}\hat{\mathcal{U}}[\hat{\xi}(\mathbf{n})]. \tag{41}$$

We observe that the effects of the hole and intrinsic nonlinearity on magnon excitations are incorporated into the factors L' and $(\lambda/2\eta)\hat{\mathcal{U}}[\hat{\xi}(\mathbf{n})]$, respectively. In studying solutions to Eq. (41), we first pay particular attention to the case, in which the energy eigenvalue E appears outside the linear spin-wave band $E^{(lsw)}$ caused by hole existence. For this purpose, we introduce a 2×2 magnon Green's-function matrix $\hat{g}(\mathbf{n})$ associated with linear magnon of the system defined by

$$\hat{L}_0\hat{g}(\mathbf{n})=\begin{bmatrix}\Delta(\mathbf{n}) & 0\\ 0 & \Delta(\mathbf{n})\end{bmatrix}. \tag{42}$$

In the component representation of $\hat{g}(\mathbf{n})(=\hat{L}_0^{-1})$ is written as

$$g_{ik}(n_x,n_y;E)=\frac{1}{N}\sum_{q_x}\sum_{q_y}\frac{b_{ik}\exp[i(q_xn_x+q_yn_y)]}{E^{(lsw)2}(q)-E^2},\quad i,k=1,2, \tag{43}$$

with

$$b_{11}=2+D^*+\overline{E},\quad b_{22}=2+D^*-\overline{E},$$

$$b_{12}=b_{21}=-\eta\sum_{j=x,y}\cos(q_j). \tag{44}$$

The reduced eigenvalue is given by

$$\overline{E}^{(lsw)2}(\mathbf{q})=(2+D^*)^2-\eta^2\left(\sum_{j=x,y}\cos(q_j)\right)^2. \tag{45}$$

The spin-wave bottom $\overline{E}_0^{(lsw)}$ is given by

$$\overline{E}_0^{(lsw)2}=(2+D^*)^2-4\eta^2. \tag{46}$$

After lengthy, though straightforward, calculations, concrete expressions for $g_{ik}(n_x,n_y;E)$ can be written in terms of the Bessel functions of imaginary arguments

$$I_n(t)=\frac{i^{-n}}{2\pi}\int_{-\pi}^{\pi}\exp[in\xi+t\cos\xi]d\xi, \tag{47}$$

as

$$g(n_x,n_y)=\frac{1}{\eta}\int_0^{\infty}dt\,e^{-\varepsilon t}I_{n_x}(t)I_{n_y}(t). \tag{48}$$

In what follows, the implementation of the method as given above is presented for case (ii) and case (iii) in succession.

IV. NUMERICAL CALCULATIONS

A. Linear defect modes

In terms of the $g_{ik}(\boldsymbol{n})$'s, Eq. (26) and Eq. (27) are rewritten as

$$\xi(\boldsymbol{n})=\sum_{\boldsymbol{l}}\{g_{11}(\boldsymbol{n}-\boldsymbol{l})W_1(\xi(\boldsymbol{0}),\zeta)+g_{12}(\boldsymbol{n}-\boldsymbol{l})W_2(\zeta(\pm\boldsymbol{e}_j),\xi)\}, \tag{49}$$

$$\zeta(\boldsymbol{m})=\sum_{\boldsymbol{l}}\{g_{21}(\boldsymbol{m}-\boldsymbol{l})W_1(\xi(\boldsymbol{0}),\zeta)+g_{22}(\boldsymbol{m}-\boldsymbol{l})W_2(\zeta(\pm\boldsymbol{e}_j),\xi)\}. \tag{50}$$

Since $W_1(\xi(\boldsymbol{l}),\zeta)$ and $W_2(\zeta(\boldsymbol{l}),\xi)$ are nonvanishing only for $\boldsymbol{l}=\boldsymbol{0}$ and $\pm\boldsymbol{e}_j$, respectively [see Eqs. (33) and (34)], substituting (0,0) for $\boldsymbol{n}$ and (1,0) for $\boldsymbol{m}$ into Eqs. (49) and (50), we obtain simultaneous equations for $\xi(0,0)$ and $\zeta(1,0)$ as follows:

$$\xi(0,0)=g_{11}(0,0)W_1(\xi(0,0),\zeta)+4g_{12}(1,0)W_2(\zeta(1,0),\xi), \tag{51}$$

$$\zeta(1,0)=g_{21}(1,0)W_1(\xi(0,0),\zeta)+[g_{22}(0,0)+2g_{22}(1,1)+g_{22}(2,0)]W_2(\zeta(1,0),\xi). \tag{52}$$

In derivation these Eqs. (51) and (52) we use the symmetry respect to the origin for an *s*-like mode. The energy $\overline{E^{(linear)}}$ of localized linear spin-wave modes with the hole is obtained from following equation though ε dependence of $g_{ik}(\boldsymbol{n})$ [see Eq. (48)],

$$\left(1-\frac{2+D^*}{\eta}g_{11}(0,0)-2g_{12}(1,0)\right)\times\left(1-2g_{12}(1,0)-\frac{1}{2\eta}[g_{22}(0,0)+2g_{22}(1,1)+g_{22}(2,0)]\right)-\left(2g_{11}(0,0)+\frac{2}{\eta}g_{12}(1,0)\right)\times\left(\frac{2+D^*}{\eta}g_{12}(1,0)+\frac{1}{2}[g_{22}(0,0)+2g_{22}(1,1)+g_{22}(2,0)]\right)=0, \tag{53}$$

where we used Eqs. (33) and (34). Its η dependence is plotted for $D^*=0.3$ in Fig. 2. We note the difference of $\overline{E^{(linear)}}$ from the bottom of the magnon band $\overline{E_0^{(lsw)}}$ increases with decreasing η, i.e., the system tends to the Ising type. This tendency is seen regardless of D^* value.

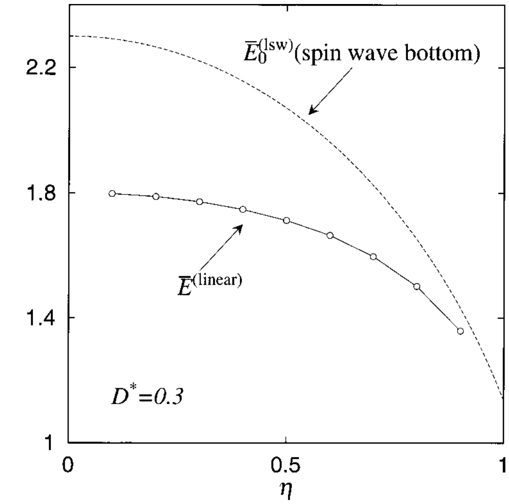

FIG. 2. η dependence of the energy eigenvalue $\overline{E^{(linear)}}$ for linear localized mode with the hole effect. This eigenvalue is lying below spin-wave bottom $\overline{E_0^{(lsw)}}$ without hole effect with $D^*=0.3$.

B. Nonlinear defect modes

To seek *s*-like nonlinear localized modes in the 2D antiferromagnet containing a hole, we introduce another 2×2 magnon Green's function $\hat{G}(\boldsymbol{n};\boldsymbol{m})$, which satisfies the following equation:

$$(\hat{L}_0-\hat{L}')\hat{G}(\boldsymbol{n};\boldsymbol{m})=\begin{bmatrix}\Delta(\boldsymbol{m}) & 0\\ 0 & \Delta(\boldsymbol{m})\end{bmatrix}. \tag{54}$$

Referring to Eqs. (20) and (21) with $\mathcal{U}_1=\mathcal{U}_2=0$, $\hat{G}(\boldsymbol{n};\boldsymbol{m})$ can be written as

$$\hat{G}(\boldsymbol{n};\boldsymbol{m})=\hat{L}_0^{-1}+\hat{L}_0^{-1}\hat{L}'\hat{G}(\boldsymbol{n};\boldsymbol{m})=\hat{L}_0^{-1}+\sum_{\boldsymbol{l}}\hat{L}_0^{-1}\hat{W}(\hat{G}(\boldsymbol{l};\boldsymbol{m})), \tag{55}$$

where we used Eq. (36). Explicit expressions for the matrix elements of $\hat{W}(\hat{G}(\boldsymbol{l};\boldsymbol{m}))$ are written down.

$$W_{11}(\hat{G}(\boldsymbol{0};\boldsymbol{m}))=(2+D^*)G_{11}(\boldsymbol{0};\boldsymbol{m})+\frac{\eta}{2}\sum_{j=x,y}[G_{21}(\boldsymbol{e}_j;\boldsymbol{m})+G_{21}(-\boldsymbol{e}_j;\boldsymbol{m})], \tag{56}$$

$$W_{12}(\hat{G}(\boldsymbol{0};\boldsymbol{m}))=(2+D^*)G_{12}(\boldsymbol{0};\boldsymbol{m})+\frac{\eta}{2}\sum_{j=x,y}[G_{22}(\boldsymbol{e}_j;\boldsymbol{m})+G_{22}(-\boldsymbol{e}_j;\boldsymbol{m})], \tag{57}$$

$$W_{21}(\hat{G}(\pm\boldsymbol{e}_j;\boldsymbol{m}))=\frac{\eta}{2}G_{11}(0;\boldsymbol{m})+\frac{1}{2}G_{21}(\pm\boldsymbol{e}_j;\boldsymbol{m}), \tag{58}$$

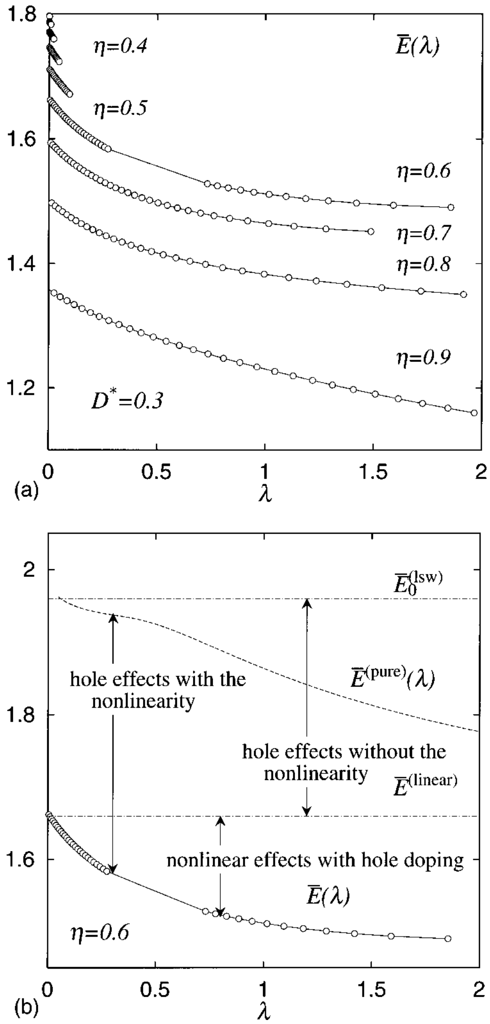

FIG. 3. (a) The energy eigenvalue $\overline{E}(\lambda)$ of an s-like self-localized mode as a function of nonlinearity parameter λ for various anisotropic exchange interaction parameters with $D^*=0.3$. (b) Illustration of energy reduction under two effects, i.e., intrinsic nonlinearity and extrinsic hole doping in a case of $\eta=0.1$. A solid line is $\overline{E}(\lambda)$ and a dashed line is the $\overline{E}^{(pure)}(\lambda)$.

$$W_{22}(\hat{G}(\pm \boldsymbol{e}_j;\boldsymbol{m}))=\frac{\eta}{2}G_{12}(0;\boldsymbol{m})+\frac{1}{2}G_{22}(\pm \boldsymbol{e}_j;\boldsymbol{m}), \quad (59)$$

$$W_{ik}(\hat{G}(\boldsymbol{l};\boldsymbol{m}))=0 \quad \text{for } |\boldsymbol{l}|>1 \quad i,k=1,2. \quad (60)$$

By using $\hat{g}(\boldsymbol{n})$, $\hat{G}(\boldsymbol{n};\boldsymbol{m})$ in Eq. (55) is re-expressed in the form

$$\hat{G}(\boldsymbol{n};\boldsymbol{m})=\hat{g}(\boldsymbol{n}-\boldsymbol{m})+\sum_{\boldsymbol{l}} \hat{g}(\boldsymbol{n}-\boldsymbol{l})\hat{W}(\hat{G}(\boldsymbol{l};\boldsymbol{m})). \quad (61)$$

Inserting Eqs. (56)–(60) into Eq. (61) leads to the explicit expression for the Green's function $G(\boldsymbol{n};\boldsymbol{m})$ (see Appendix). Corresponding to Eqs. (49) and (50) in the linear defect, the envelope functions of nonlinear self-localized mode are obtained as

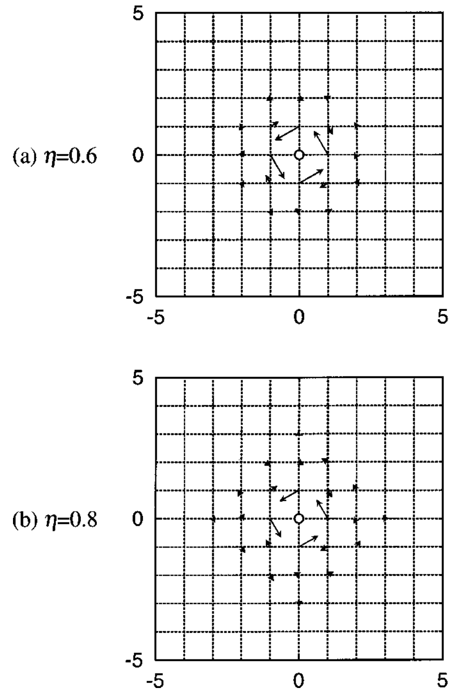

FIG. 4. The projection of spin profile of an s-like self-localized mode $\boldsymbol{S}_n$ on a xy plane. (a) $\eta=0.6$ with $\overline{E}=1.54$ and $\lambda=0.612$; (b) $\eta=0.8$ with $\overline{E}=1.45$ and $\lambda=0.219$.

$$\xi(\boldsymbol{n})=\frac{\lambda}{2\eta}\sum_{m} G_{11}(\boldsymbol{n};\boldsymbol{m})\mathcal{U}_1(\xi(\boldsymbol{m}),\zeta(\boldsymbol{m})) + G_{12}(\boldsymbol{n};\boldsymbol{m})\mathcal{U}_2(\zeta(\boldsymbol{m}),\xi(\boldsymbol{m})), \quad (62)$$

$$\zeta(\boldsymbol{n})=\frac{\lambda}{2\eta}\sum_{m} G_{21}(\boldsymbol{n};\boldsymbol{m})\mathcal{U}_1(\xi(\boldsymbol{m}),\zeta(\boldsymbol{m})) + G_{22}(\boldsymbol{n};\boldsymbol{m})\mathcal{U}_2(\zeta(\boldsymbol{m}),\xi(\boldsymbol{m})). \quad (63)$$

Since the profile functions $\xi(\boldsymbol{n})$ and $\zeta(\boldsymbol{n})$ are scaled by the amplitude $\mathcal{A}/\sqrt{2S}$ [see Eqs. (18) and (19)] let us regard $\zeta(\pm \boldsymbol{e}_j)$ as unity. This normalization condition can be written as

$$\zeta(\pm \boldsymbol{e}_j)=\frac{\lambda}{2\eta}\sum_{m}\{G_{21}(\boldsymbol{e}_j,\boldsymbol{m})\mathcal{U}_1(\xi,\zeta)+G_{22}(\boldsymbol{e}_j,\boldsymbol{m})\mathcal{U}_2(\zeta,\xi)\} =1. \quad (64)$$

By using Eq. (64), Eqs. (62) and (63) are replaced to

$$\xi(\boldsymbol{n})=\frac{\sum_{m} G_{11}(\boldsymbol{n},\boldsymbol{m})\mathcal{U}_1(\xi,\zeta)+G_{12}(\boldsymbol{n},\boldsymbol{m})\mathcal{U}_2(\zeta,\xi)}{\sum_{m} G_{21}(\pm \boldsymbol{e}_j;\boldsymbol{m})\mathcal{U}_1(\xi,\zeta)+G_{22}(\pm \boldsymbol{e}_j;\boldsymbol{m})\mathcal{U}_2(\xi,\zeta)}, \quad (65)$$

$$\zeta(\boldsymbol{n})=\frac{\sum_{m} G_{21}(\boldsymbol{n},\boldsymbol{m})\mathcal{U}_1(\xi,\zeta)+G_{22}(\boldsymbol{n},\boldsymbol{m})\mathcal{U}_2(\zeta,\xi)}{\sum_{m} G_{21}(\pm\boldsymbol{e}_j;\boldsymbol{m})\mathcal{U}_1(\xi,\zeta)+G_{22}(\pm\boldsymbol{e}_j;\boldsymbol{m})\mathcal{U}_2(\xi,\zeta)}. \tag{66}$$

Insertion of above formal solutions for $\xi(\boldsymbol{n})$ and $\zeta(\boldsymbol{n})$ with $\zeta(\boldsymbol{e}_x)=1$ into Eq. (64) yields a relationship between ε and λ in an implicit form. The numerical calculation was carried out under the same procedure as that in the previous paper.[1]

In Fig. 3(a), the energy eigenvalue $\overline{E}$ of the self-localized s-like nonlinear modes is plotted against to λ for various values of η for $D^*=0.3$. Increase of the nonlinear parameter λ leads to the lowering of $\overline{E}$. In Fig. 3(b), it is illustrated for $\eta=0.6$ how the eigenvalue E decreases under two effects, i.e., intrinsic nonlinearity and the the extrinsic spatially inhomogeneous due to the hole existence. For reference $\overline{E^{(pure)}}$ is also shown, which is the energy eigenvalue for the pure system without hole but including nonlinear effect.

Since the diagonal coherent-state representation of spin operator $\boldsymbol{S}_n$ is given in terms of the profile functions $\xi(\boldsymbol{n})$ and $\zeta(\boldsymbol{m})$ [see Eqs. (4), (18), and (19)], the projections of $\boldsymbol{S}_n$ on the 2D square lattice plane, denoted $\boldsymbol{S}_n^{\perp}$, can be evaluated. In Fig. 4 the obtained results are drawn for two cases (a) $\eta=0.6$ and (b) $\eta=0.8$ with given values of λ and E and $D^*=0.3$. In the case of $\eta=0.6$, $\boldsymbol{S}_n^{\perp}$ appear to be large in the magnitude around a hole site $\boldsymbol{n}=\boldsymbol{0}$ and its direction is indicated by arrows. This is so-called localized magnetic vortex. This implies that the spins in the neighborhood of a hole undergo a large excursion, whereas the spin deviation of the rest is very small. This localized magnetic vortex seems to be peculiarity in 2D nonlinear spin system associated with a hole. As the system shifts to Heisenberg type, the spin deviated region spreads out surrounding the hole but the magnitudes of $\boldsymbol{S}_n^{\perp}$ become smaller than the former case as shown in Fig. 4(b).

V. CONCLUDING REMARKS

In this paper, we have developed a theory of nonlinear self-localized modes in 2D square anisotropic Heisenberg antiferromagnets containing a fixed magnetic hole in the same spirit as that in previous ferromagnetic paper. Since the present system is composed of two interpenetrating sublattice A and B, the uniaxial anisotropy energy D is indispensable for the formation of localized mode. The result obtained in this paper is summarized as follows. In contrast with the case of the ferromagnet where both of immobile and mobile nonlinear modes are shown to exist, we could not found any trace of moving modes. In the case of immobile nonlinear modes, the appearance of vortexlike modes around a hole with energy lying below the linear spin-wave energy band is found. It turns out that the intrinsic nonlinearity tends to stabilize the magnetic localized mode generated by the extrinsic hole doping in the sense that lowering of the energy E is enhanced by increasing nonlinearity parameter λ. Physically, the appearance of the stationary localized mode due to hole doping and the nonlinearity implies local destruction of the antiferromagnetic state.

APPENDIX: DERIVATION OF GREEN'S FUNCTION FOR GENERAL SITES

Inserting Eqs. (56)–(60) to Eq. (61), the elements of Green's functions $G_{ik}(\boldsymbol{n};\boldsymbol{m})$ are written as follows:

(i) for $n_x+n_y=$ even,

$$\begin{aligned}G_{11}(\boldsymbol{n};\boldsymbol{m})={}&g_{11}(\boldsymbol{n}-\boldsymbol{m})+[\Delta(\boldsymbol{n})+\overline{E}g_{11}(\boldsymbol{n})]G_{11}(\boldsymbol{0};\boldsymbol{m})\\&+\frac{1}{2}g_{11}(\boldsymbol{n})\sum_{j=x,y}[G_{21}(\boldsymbol{e}_j;\boldsymbol{m})+G_{21}(-\boldsymbol{e}_j;\boldsymbol{m})]\\&+\frac{1}{2\eta}\sum_{j=x,y}[g_{12}(\boldsymbol{n}-\boldsymbol{e}_j)G_{21}(\boldsymbol{e}_j;\boldsymbol{m})\\&+g_{12}(\boldsymbol{n}+\boldsymbol{e}_j)G_{21}(-\boldsymbol{e}_j;\boldsymbol{m})],\end{aligned} \tag{A1}$$

$$\begin{aligned}G_{12}(\boldsymbol{n};\boldsymbol{m})={}&g_{12}(\boldsymbol{n}-\boldsymbol{m})+[\Delta(\boldsymbol{n})+\overline{E}g_{11}(\boldsymbol{n})]G_{12}(\boldsymbol{0};\boldsymbol{m})\\&+\frac{1}{2}g_{11}(\boldsymbol{n})\sum_{j=x,y}[G_{22}(\boldsymbol{e}_j;\boldsymbol{m})+G_{22}(-\boldsymbol{e}_j;\boldsymbol{m})]\\&+\frac{1}{2\eta}\sum_{j=x,y}[g_{12}(\boldsymbol{n}-\boldsymbol{e}_j)G_{22}(\boldsymbol{e}_j;\boldsymbol{m})\\&+g_{12}(\boldsymbol{n}+\boldsymbol{e}_j)G_{22}(-\boldsymbol{e}_j;\boldsymbol{m})],\end{aligned} \tag{A2}$$

$$G_{21}(\boldsymbol{n};\boldsymbol{m})=g_{21}(\boldsymbol{n}-\boldsymbol{m}), \tag{A3}$$

$$G_{22}(\boldsymbol{n};\boldsymbol{m})=g_{22}(\boldsymbol{n}-\boldsymbol{m}), \tag{A4}$$

(ii) for $n_x+n_y=$ odd,

$$G_{11}(\boldsymbol{n};\boldsymbol{m})=g_{11}(\boldsymbol{n}-\boldsymbol{m}), \tag{A5}$$

$$G_{12}(\boldsymbol{n};\boldsymbol{m})=g_{12}(\boldsymbol{n}-\boldsymbol{m}), \tag{A6}$$

$$\begin{aligned}G_{21}(\boldsymbol{n};\boldsymbol{m})={}&g_{21}(\boldsymbol{n}-\boldsymbol{m})+\overline{E}g_{21}(\boldsymbol{n})G_{11}(\boldsymbol{0};\boldsymbol{m})\\&+\frac{1}{2}g_{21}(\boldsymbol{n})\sum_{j=x,y}[G_{21}(\boldsymbol{e}_j;\boldsymbol{m})+G_{21}(-\boldsymbol{e}_j;\boldsymbol{m})]\\&+\frac{1}{2\eta}\sum_{j=x,y}[g_{22}(\boldsymbol{n}-\boldsymbol{e}_j)G_{21}(\boldsymbol{e}_j;\boldsymbol{m})\\&+g_{22}(\boldsymbol{n}+\boldsymbol{e}_j)G_{21}(-\boldsymbol{e}_j;\boldsymbol{m})],\end{aligned} \tag{A7}$$

$$\begin{aligned}G_{22}(\boldsymbol{n};\boldsymbol{m})={}&g_{22}(\boldsymbol{n}-\boldsymbol{m})+\overline{E}g_{21}(\boldsymbol{n})G_{12}(\boldsymbol{0};\boldsymbol{m})\\&+\frac{1}{2}g_{21}(\boldsymbol{n})\sum_{j=x,y}[G_{22}(\boldsymbol{e}_j;\boldsymbol{m})+G_{22}(-\boldsymbol{e}_j;\boldsymbol{m})]\\&+\frac{1}{2\eta}\sum_{j=x,y}[g_{22}(\boldsymbol{n}-\boldsymbol{e}_j)G_{22}(\boldsymbol{e}_j;\boldsymbol{m})\\&+g_{22}(\boldsymbol{n}+\boldsymbol{e}_j)G_{22}(-\boldsymbol{e}_j;\boldsymbol{m})].\end{aligned} \tag{A8}$$

Thus we obtain a set of equations respect to following ten kinds of magnon Green's function:

$$\begin{pmatrix} G_{11}(0,0;\boldsymbol{m}) & G_{12}(0,0;\boldsymbol{m}) & & \\ G_{21}(1,0;\boldsymbol{m}) & G_{21}(0,1;\boldsymbol{m}) & G_{21}(-1,0;\boldsymbol{m}) & G_{21}(0,-1;\boldsymbol{m}) \\ G_{22}(1,0;\boldsymbol{m}) & G_{22}(0,1;\boldsymbol{m}) & G_{22}(-1,0;\boldsymbol{m}) & G_{22}(0,-1;\boldsymbol{m}) \end{pmatrix}. \tag{A9}$$

By using $\hat{g}(\boldsymbol{n})$ and Eq. (61) incorporating with solutions for the above ten Green's functions, we can finally evaluate $G_{ik}(\boldsymbol{n};\boldsymbol{m})$ for general sites.

[1] M. Kubota, K. Kawasaki, and S. Takeno, Phys. Rev. B **60**, 12 810 (1999).

[2] H. Kuratsuji and T. Suzuki, J. Math. Phys. **21**, 472 (1980).

[3] R. P. Feynman and A. R. Hibbs, *Quantum Mechanics and Path Integrals* (McGraw-Hill, New York, 1965).

[4] J. R. Klauder and B. S. Skagerstam, *Coherent States. Applications in Physics and Mathematical Physics* (World Scientific, Singapore, 1985).

[5] R. K. Dodd, J. C. Eilbeck, J. D. Gibbon, and H. C. Morris, *Solitons and Nonlinear Wave Equations* (Academic Press, London, 1982).